

## Fabrication of an Electromagnetic Micropump for Cerebrospinal Fluid Shunt

金明植\* · 李士旭\*\* · 梁翔植\*\*\*  
(Myung Sik Kim · Sang Wook Lee · Sang Sik Yang)

**Abstract** This paper presents the fabrication and test of a micropump that can be applied to an implantable cerebrospinal fluid shunt system for hydrocephalus patients. The proposed micropump consists of a pair of corrugated parylene diaphragm chambers and a set of nozzle and diffuser. The electromagnetic force drives the diaphragms and pumps the fluid. The static or dynamic characteristics of the fabricated devices have been obtained experimentally. The size of the micropump is  $14 \times 12 \times 8\text{mm}^3$ . The flow rate increase by about 3 ml/h was observed in the operational pressure range of the micropump.

**Key Words** :Micropump , Electromagnetic force, Cerebrospinal Fluid Shunt

### 1. Introduction

Hydrocephalus is a neurological disease of an abnormal increment in intracranial pressure that occurs when there is an abnormal accumulation of cerebrospinal fluid (CSF) in the ventricles and/or subarachnoid space of the brain. The abnormal accumulation of CSF is attributed to an overproduction of CSF, an obstruction of the drainage of CSF, or a failure of the structures of the brain to reabsorb the fluid. A CSF shunt system drains CSF from the brain to the abdominal cavity.

A conventional CSF shunt system consists of a passive shunt valve and a tube. It adjusts flow rate depending on the patient's brain intracranial pressure. The valve opening pressure of the conventional CSF shunt system is not adjustable, and not able to manage the problem of over/underdrainage. No ideal CSF shunt system exists at present. An advanced CSF shunt system is required in order to monitor and regulate the intracranial pressure after implantation. Fig. 1 shows an intelligent closed-loop control shunt system that adjust the flow rate of a micropump implanted in a body.

Since high temperature and high voltage are not allowed in a body, the thermopneumatic type, the electrostatic type and the piezoelectric type are not suitable. The electromagnetic actuator provides a large displacement compared to the moderate power consumption. Electromagnetic microactuators with a permanent magnet and a planar coil on a Parylene diaphragm have been fabricated and tested.[1,2] The fabrication process of the planar coil, however, is very complicated.

This paper presents an implantable micropump that has a simple structure and a simple fabrication process. The electromagnetic microactuator has a solenoid and a ferromagnetic disk on a Parylene diaphragm.

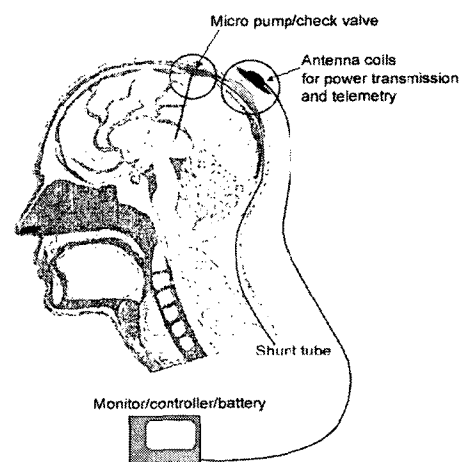


Fig. 1 The diagram of closed-loop controlled CSF shunt system.

\* 準會員：亞州大 電子工學部 碩士 (주)디지털웨이 研究員

\*\* 準會員：亞州大 機械工學部 碩士

電子部品研究院 나노 메카 實驗室 研究員

\*\*\* 正會員：亞州大 電子工學部 教授 · 工博

接受日字：2001年 12月 28日

最終完了：2002年 10月 10日

The micropump has a nozzle/diffuser instead of microvalves so that it can be easily fabricated by micromachining[3]. The fabricated micropump is tested and the characteristics of the actuator and the pump are illustrated.

## 2. Structure and Analysis

Fig. 2 shows the schematic diagram of an electromagnetic micropump. It has two chambers and micro nozzle/diffuser. The bottom substrate has cavities for solenoid coils. In the middle substrate, there are Ni/Fe permalloy disks on parylene diaphragm. The top PDMS layer has channels and pump chambers.

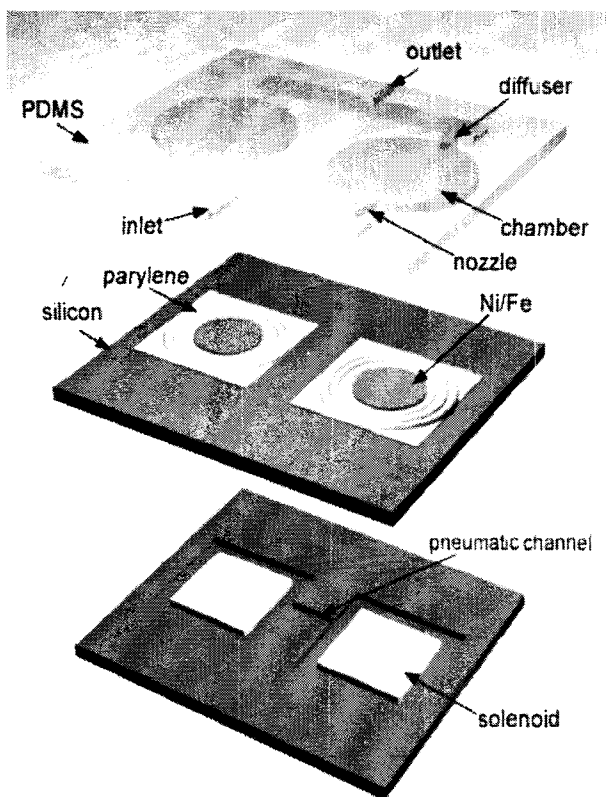


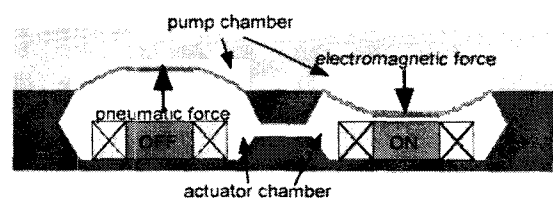
Fig. 2 A perspective view of the micro pump.

Parylene is a bio-compatible and nontoxic material. The parylene diaphragm makes relatively large displacement to low input voltage compared to metal or silicon diaphragms. The diaphragm with corrugations around the Ni/Fe alloy disk is estimated to deflect about 1.5 times than flat diaphragm for the same power consumption, which was confirmed by K. H. Kim & S. S. Yang[2]. Fig. 3 shows the actuation mechanism of the proposed micro electromagnetic pump. The actuator chambers are sealed and two chambers are connected through a pneumatic channel. When the input current is applied to one of the

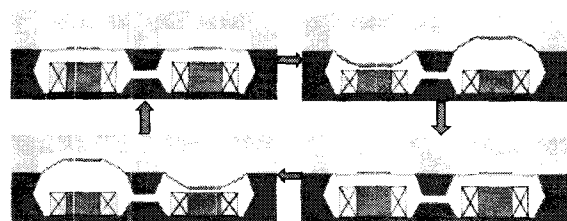
coils as shown in Fig. 3(a), the diaphragm above the coil is pulled by the electromagnetic attraction force acting on the Ni/Fe alloy disk, the other diaphragm is pushed by the pneumatic force generated by the compressed air in the actuator chambers. When the current is applied to two actuators alternately as in Fig. 3(b), two diaphragms are driven respectively in opposite directions by the electromagnetic and the pneumatic forces.

If the diaphragms move up and down, the fluid filled in the pump chambers flows out and in, respectively. Eventually, the fluid flows from the inlet to the outlet due to the flow characteristic difference[3]. The depth and the diameter of the pump chamber are respectively  $50\mu\text{m}$  and  $5\text{mm}$  so that the dead space of the chamber is minimized. The volume of each pump chamber is  $0.79\mu\text{l}$ . The diffuser length is  $1\text{mm}$  and the interior angle is  $7$  degrees. The size of the micropump is  $14 \times 12 \times 8\text{mm}^3$ .

Using FlumeCAD™, we performed the numerical analysis to investigate the flow characteristic difference between the nozzle and the diffuser. FlumeCAD is an integrated software consisting of 3D design, modeling and simulation tools for micro fluidic devices. The geometry of the current designed micropump is shown in Fig. 4. Analyses of geometry configurations were conducted to predict the pumping range and flow rate. Initial opening pressure applied to the two chambers about  $100\text{mmH}_2\text{O}$  that operational pressure range of passive shunt valve. A result of simulation, quantity and density of velocity vector of diffuser is higher than that of nozzle. It shows the suitability of designed nozzle-diffuser on the micropump.



(a)



(b)

Fig. 3 The actuation mechanism of the micro actuators. (a) The diaphragm deflection by the electromagnetic force and the pneumatic force. (b) The actuation sequence of the two actuators.

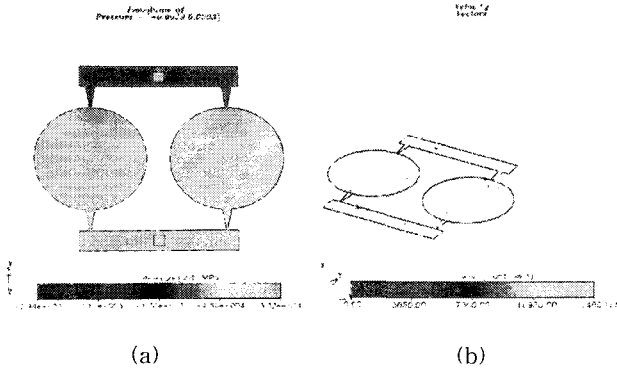


Fig. 4 Analytic result of the micropump in FlumeCAD.  
 (a) A pressure distribution view (unit: MPa)  
 (b) A fluid vector velocity view (unit:  $\mu\text{m/s}$ )

### 3. Fabrication

Fig. 5 is the fabrication process of the actuator substrate with the corrugated diaphragm. Silicon dioxide etch mask layers are grown on a  $525\ \mu\text{m}$ -thick 4 inch n-type(100) silicon wafer. For the fabrication of the cavity, the silicon oxide on the backside of the wafer is patterned and etched by  $400\ \mu\text{m}$  with the TMAH (Tetramethylammonium hydroxide) etchant. The shallow etch with EPW (Ethylendiamine : pyrocatechol : DI water =  $250\ \text{ml} : 40\ \text{g} : 80\ \text{ml}$ ) patterns the front side of the wafer with corrugations. Parylene-C is deposited by  $2.5\ \mu\text{m}$  on the front side. After the deposition, the remaining silicon under the Parylene layer is etched with EPW to obtain a Parylene diaphragm. Cr( $200\ \text{\AA}$ ) and Au( $2000\ \text{\AA}$ ) are evaporated as a seed layer for electroplating. Thick photo resistor (AZ 4620) is coated and patterned for the mold of electroplating. Ni/Fe is electroplated by  $20\ \mu\text{m}$ . Then, the photo resistor layer and the Cr/Au layer are removed sequentially. The fabricated actuator diaphragm is shown in Fig. 6.

Fig. 7 is the fabrication process of the pump chamber. The mold for the nozzle/diffuser and the chamber is fabricated on a silicon wafer with SU-8 50. Then, PDMS(Sylgard 184; Dow Corning, USA, base : curing agent = 10:1) is poured on wafer and cured for about 3 hours on  $75\ ^\circ\text{C}$ . Fig. 8 is the photograph of the pump chamber fabricated with PDMS. Fig. 9 shows the nozzle connected to pump chamber.

The enamelled wire is wound to make solenoids that are to be fitted in the cavities of the bottom substrate under the diaphragm. The Coil inductance is  $8.88\ \text{mH}$ , and the resistance is  $16\ \Omega$ . When the voltage applied to the coil is  $5\ \text{V}$ , the measured current is  $30\ \text{mA}$ . Fig. 10 shows the cross-sectional view of the assembled micro pump. Fig. 11 is the photograph of the assembled micropump.

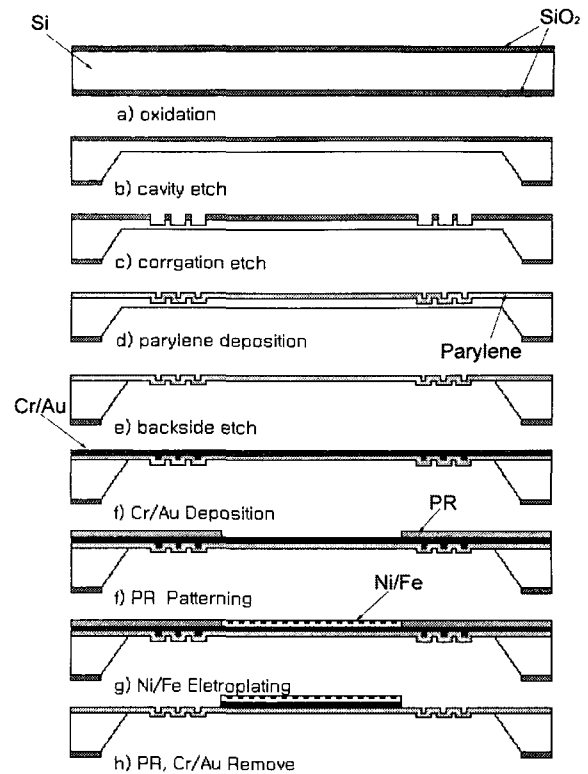


Fig. 5 The fabrication process of the diaphragm.

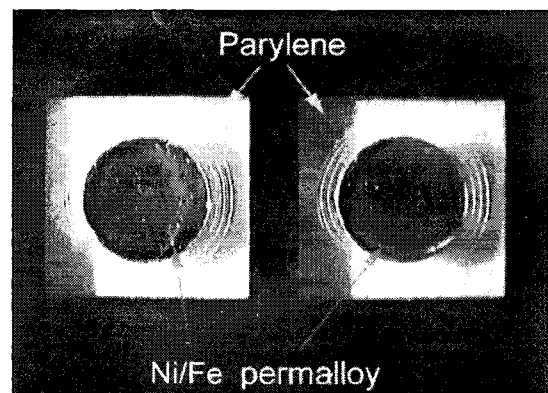


Fig. 6 The photograph of the fabricated diaphragm.

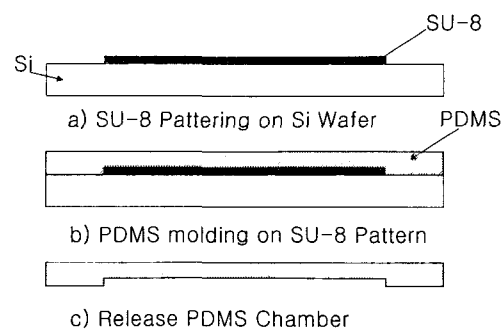


Fig. 7 The fabrication process of the pump chambers.

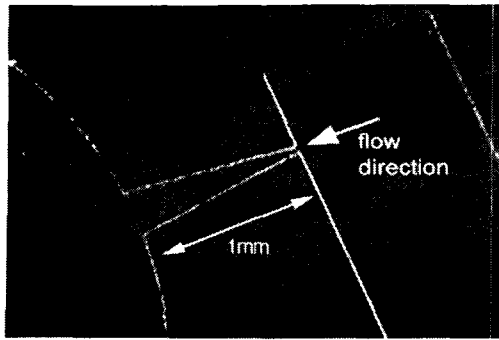


Fig. 8 The photograph of the fabricated nozzle at the pump chamber inlet.

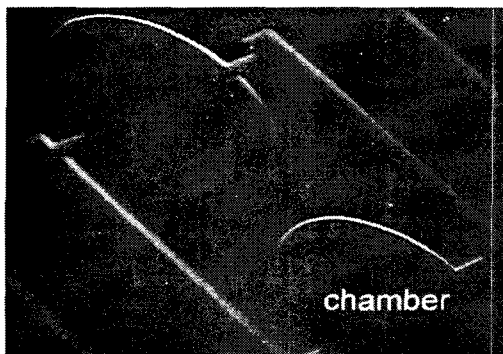


Fig. 9 The photograph of the pump chamber fabricated with PDMS.

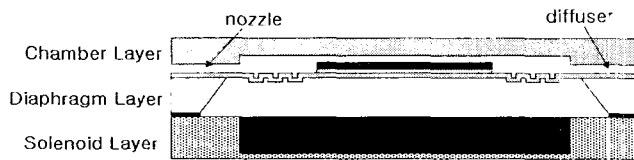


Fig. 10 The cross-sectional view of the assembled micro pump.

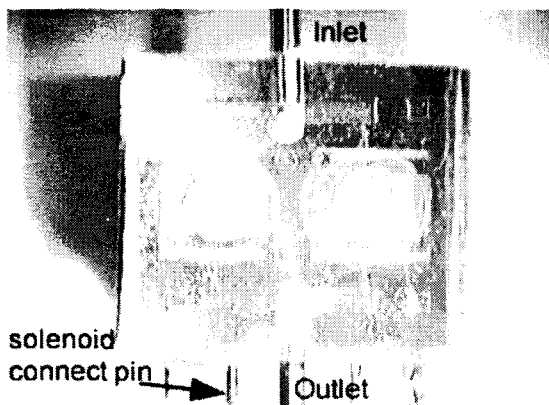


Fig. 11 The photograph of the assembled micropump.

#### 4. Test

The diaphragm characteristic test consists of the static and the dynamic deflection tests. The measurement setup of the static deflection of the diaphragm is shown in Fig. 12. The diaphragm deflections to various static pressures applied are measured with a laser displacement meter (KEYENCE LC-2420). Fig. 13 shows the diaphragm deflection vs. the applied pressure. The deflection increases as the applied pressure increases and the slope changes around 300 mmH<sub>2</sub>O.

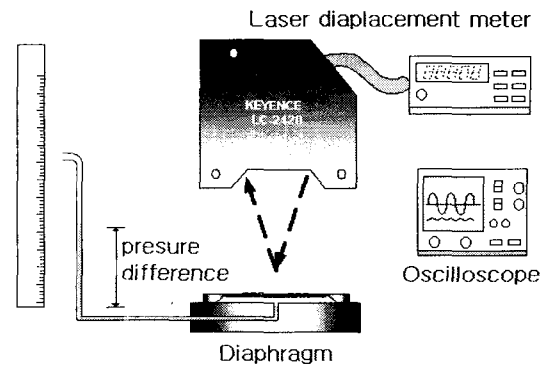


Fig. 12 The measurement setup for the static characteristic of the diaphragm.

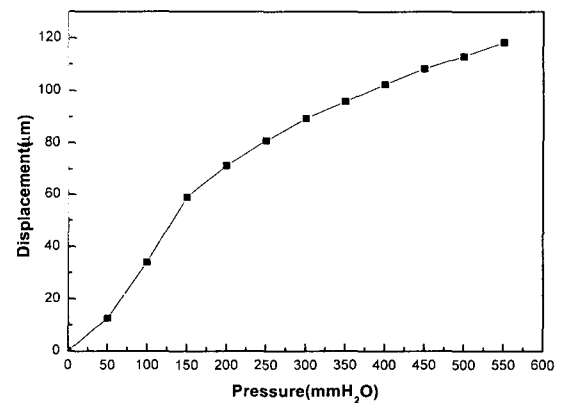


Fig. 13 The diaphragm deflection for the applied pressure.

Fig. 14 shows the measurement setup of the dynamic deflection of the diaphragm. The center displacement of the diaphragm to input current at various frequencies was measured with a laser displacement meter. Fig. 15 shows the frequency responses of the diaphragm. As the input current increases, the displacement increases. As the input frequency increases, the displacement decreases. The estimated cut-off frequency is about 10 Hz. When the applied input currents are 20 and 30mA, the maximum diaphragm displacements are 35 $\mu$ m and 40 $\mu$ m, respectively.

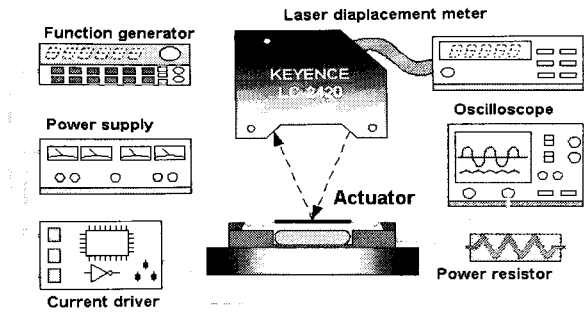


Fig. 15 The measurement setup for the dynamic characteristic of the diaphragm.

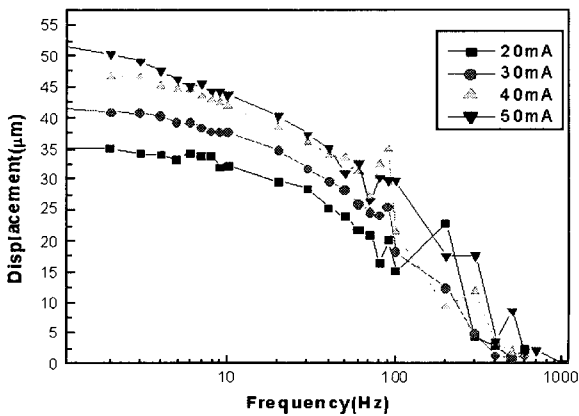


Fig. 16 The frequency response of the diaphragm.

Fig. 16 illustrates the measurement setup of the flow characteristics of the fabricated micropump. Tubes are connected to the inlet and the outlet of the micropump. The flow rate is measured under the static pressure difference. Fig. 17 shows the plot of the measured flow rate vs. frequency for two input voltages at the pressure of 0 mmH<sub>2</sub>O. The maximum flow rate of the micropump is about 6 ml/h at 3Hz when the input voltage is 9V.

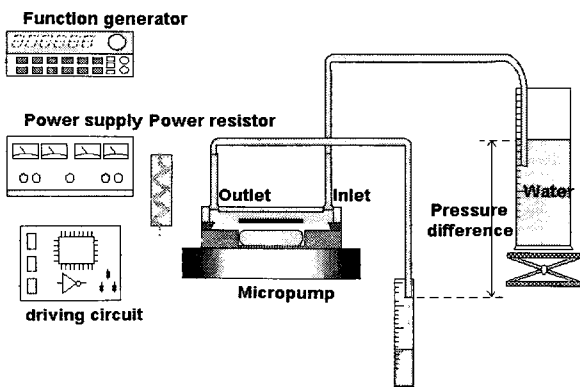


Fig. 17 The measurement setup for the flow rate of the micropump.

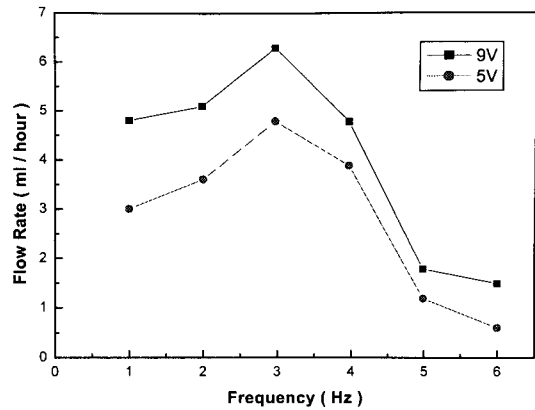


Fig. 18 Measured flow rates of the two micropumps.

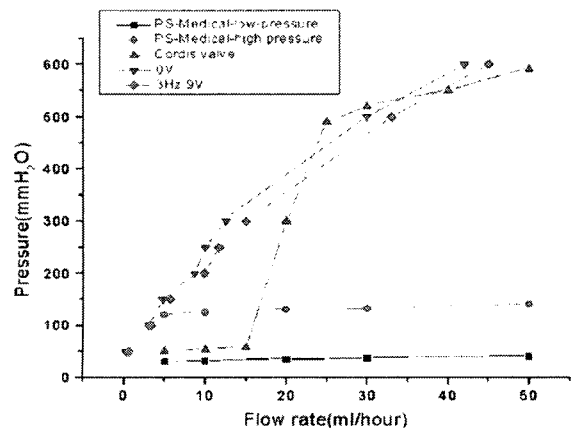


Fig. 19 The characteristics curve of pressure vs. flow rate (compared conventional valves).

Fig.18 illustrates the flow characteristics of the fabricated micropump and two typical commercialized shunt valves. Obviously, the flow rate of the fabricated micropump is comparable to that of the Cordis™ valve in the working pressure range corresponding to the intracranial pressure. By applying input voltage of 9 V, the flow rate is increased by about 3 ml/h. In the low pressure region, the flow rate of the micropump is somewhat less than the Cordis valve, but the flow rate can be increased by the adjustment of the nozzle/diffuser size.

### 5. Conclusion

In this paper, the electromagnetic micropump for an implantable CSF shunt system was proposed. The micropump has two chambers with the nozzle/diffuser. The solenoid actuates the flexible Parylene diaphragm with the Ni/Fe alloy disk on. The numerical calculation result illustrates the effectiveness of the nozzle/diffuser. The micropump was fabricated by micromachining. The static

and the dynamic characteristic tests for the fabricated diaphragm were performed. The frequency at which the maximum flow rate of the pump is achieved is 3 Hz. It is illustrated that the flow rate is increased by 3 ml/h when the pump is operated with 9 V. The test result confirms that the fabricated micropump is feasible for the CSF shunt system.

In the near future, a closed loop system which regulates the intracranial pressure by adopting the micropump developed in this paper will be completed and in-vitro test will be carried out.

**감사의 글**

This study was supported by a grant of the Good Health 21 R&D Project, Ministry of Health & Welfare, Republic of Korea. (HMP-99-E-12-0005)

**참고 문헌**

- [1] H. G. Jeong, O. C. Jeong, S. Yang, "Fabrication of electromagnetic microactuator with an electroplated coil on a parylene diaphragm," Proc. of SPIE's 7th International Symposium on Smart Structures and Materials, Vol. 3990, pp. 272-280, 2000. 3.
- [2] K. H. Kim, S. S. Yang, "Fabrication and Test of an Electromagnetic Micro Actuator with a Planar Coil on a Parylene Diaphragm," The 2000 ASME IMECE, Orlando, U.S.A., MEMS-Vol.2, pp. 281-286, 2000. 11.
- [3] Anders Olsson, C., "Valve-Less Diffuser Micropumps Fabricated using Thermoplastic Replication" Proceeding IEEE International Conference on Micro Electro Mechanical Systems, Vol. 39, pp. 517 - 521, 1990.

**저 자 소 개**



**김 명 식(金明植)**

1977년 3월 10일 생. 2002년 아주대 전자공학과 졸업(석사). 현재 (주) 디지털웨이 연구원

E-mail : mskim\_77@hotmail.com



**이 상 옥(李相旭)**

1971년 3월 29일 생. 2001년 아주대 기계공학과 졸업(석사). 현재 전자부품연구원 나노메카 실험실 연구원

E-mail:judas1951@lycos.co.kr



**양 상 식(梁翔植)**

1958년 1월 16일 생. 1980년 서울대 공대 기계공학과 졸업(석사). 1983년 동대학원 기계공학과 졸업(공학박). New jersey Institute of Technology 연구 조교수. 현재 아주대 공대 전자공학부 교수.

주관심 분야: 마이크로 소자의 Mechanism과 Actuation, Motion Control과 Nonlinear Control  
Tel: 031-219-2481, Fax:031-212-9531  
E-mail: ssyang@madang.ajou.ac.kr